Analysis of Guided Waves Along the Cladded Optical Fiber: Parabolic-Index Core and Homogeneous Cladding

MASAHIRO HASHIMOTO, MEMBER, IEEE, SHOJIRO NEMOTO, AND TOSHIO MAKIMOTO, MEMBER, IEEE

***Abstract*—This paper is concerned with the determination of the propagation characteristics of modes in the cladded optical fiber which consists of a parabolic-index core and a uniform cladding. The propagation constants of propagating modes are obtained analytically. The results are given in simple form. The asymptotic forms of the propagation constants are also given, which are valid for lower order mode propagation.**

I. Introduction

The propagation characteristics of propagating modes in the cladded parabolic-index optical fiber may be determined from the solutions of Maxwell's equations subject to certain boundary conditions. This problem can be reduced to the problem of solving the characteristic equation which is derived by matching the physically admissible solutions in core and cladding at the core boundary. The Kurtz–Streifer approximation [1], [2] may be useful in obtaining the approximate core solutions (the vector modes [3]). With such an approximation, Yamada and Inabe [4] have derived the characteristic equation. However, the mathematical form of such an equation is not suited to the computation of the propagation constants; numerical techniques are required.

The purpose of this paper is to show that the characteristic equation can be solved approximately using the field decomposition approach previously developed in two-dimensional cases [5], [6]. The formulas derived for the propagation constants are simple in form. The asymptotic formulas are also given, which are applicable for lower order modes.

II. Exact Characteristic Equation

A. Field Components

The refractive-index variation of the cladded optical fiber considered here is (see Fig. 1)

$$n(r) = n_0\sqrt{1-\chi(r)} \tag{1}$$

where n_0 is the refractive index on the center axis (the z axis), and $\chi(r)$ is the truncated parabolic function defined by the parabolic function when r is less than the core radius a and the constant δ when r exceeds a,

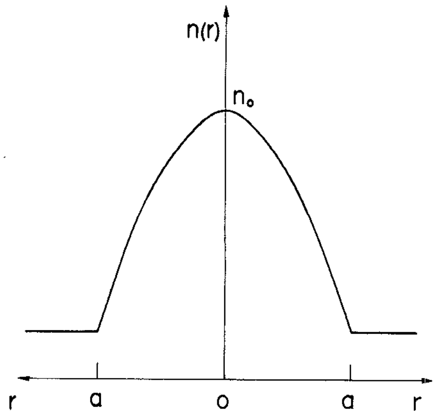

Fig. 1. Refractive-index profile of the cladded optical fiber.

$$\chi(r) \equiv \begin{cases} \delta(r/a)^2, & \text{for } r < a \\ \delta, & \text{for } r \geq a. \end{cases} \tag{2}$$

This means that the refractive index of the homogeneous cladding is $n_0\sqrt{1-\delta}$. In such a waveguide (a cladded optical fiber), the electric and magnetic field components are written as[1]

$$\begin{aligned}
E_z &= U(r)e^{jm\theta - j\beta z} \\
H_z &= -jY_0V(r)e^{jm\theta - j\beta z} \\
E_r &= \frac{1}{jk(b-\chi)}\left\{\sqrt{1-b}\,U'(r) + \frac{m}{r}V(r)\right\} e^{jm\theta - j\beta z} \\
E_\theta &= \frac{1}{k(b-\chi)}\left\{V'(r) + \sqrt{1-b}\,\frac{m}{r}U(r)\right\} e^{jm\theta - j\beta z} \\
H_r &= -\frac{Y_0}{k(b-\chi)}\left\{\sqrt{1-b}\,V'(r) + (1-\chi)\frac{m}{r}U(r)\right\} \cdot e^{jm\theta - j\beta z} \\
H_\theta &= \frac{Y_0}{jk(b-\chi)}\left\{(1-\chi)U'(r) + \sqrt{1-b}\,\frac{m}{r}V(r)\right\} \cdot e^{jm\theta - j\beta z}
\end{aligned} \tag{3}$$

where m is an integer, k is the wave number on the z axis, Y_0 is the wave admittance ($= k/\omega\mu_0$) on the z axis, β is

Manuscript received March 3, 1976; revised June 2, 1976.
M. Hashimoto was with the Communication Research and Development Department, Communication Equipment Works, Mitsubishi Electric Corporation, Amagasaki 661, Japan. He is now with the Department of Applied Electronic Engineering, Osaka Electro-Communication University, Neyagawa, Osaka 572, Japan.
S. Nemoto and T. Makimoto are with the Department of Electrical Engineering, Osaka University, Toyonaka 560, Japan.

[1] Equations (3) and (5) are cited from [1] and [4] with different symbols. The readers should be careful not to confuse symbols when they refer to earlier publications.

the propagation constant, and b is the unknown parameter which is associated with β by

$$\beta = k\sqrt{1-b}. \tag{4}$$

Therefore, we determine the parameter b instead of β. The functions $U(r)$ and $V(r)$ are related with each other through the coupled differential equations

$$U''(r) + \left(\frac{1}{r} + \frac{\chi'}{b-\chi} - \frac{\chi'}{1-\chi}\right) U'(r) + \left[k^2(b-\chi) - \frac{m^2}{r^2}\right] U(r) = -m\sqrt{1-b}\left(\frac{1}{1-\chi}\right)\left(\frac{\chi'}{b-\chi}\right)\frac{V(r)}{r}$$

$$V''(r) + \left(\frac{1}{r} + \frac{\chi'}{b-\chi}\right) V'(r) + \left[k^2(b-\chi) - \frac{m^2}{r^2}\right] V(r) = -m\sqrt{1-b}\left(\frac{\chi'}{b-\chi}\right)\frac{U(r)}{r} \tag{5}$$

where $\chi' \equiv d\chi/dr$.

B. Fields in the Core and the Cladding

The vector modes in an uncladded optical fiber are called TE waves and TM waves for $m = 0$, and HE waves and EH waves for $m \geq 1$ [3]. According to this classification, we write the bounded solutions of (5) in the core region as

$$\{U(r),V(r)\} = \begin{cases} \{0,V_1(r)\}, & \text{for TE waves} \\ \{U_2(r),0\}, & \text{for TM waves} \\ \{U_1(r),V_1(r)\}, & \text{for HE waves} \\ \{U_2(r),V_2(r)\}, & \text{for EH waves} \end{cases} \tag{6}$$

while, in the cladding region, we find two types of waves

$$\{U(r),V(r)\} = \begin{cases} \{0,V_3(r)\}, & \text{for TE waves} \\ \{U_3(r),0\}, & \text{for TM waves} \end{cases} \tag{7}$$

where

$$U_3(r) = V_3(r) = K_m(k\sqrt{\delta - b}\, r) \tag{8}$$

and K_m is the modified Bessel function of mth order.

C. Matching Conditions at $r = a$

The fields in the core region and the cladding region are represented by the linearly combined forms

$$\left.\begin{aligned} U(r) &= AU_1(r) + BU_2(r) \\ V(r) &= AV_1(r) + BV_2(r) \end{aligned}\right\}, \quad 0 \leq r \leq a$$
$$\left.\begin{aligned} U(r) &= -CU_3(r) \\ V(r) &= -DU_3(r) \end{aligned}\right\}, \quad a \leq r \leq \infty \tag{9}$$

respectively, where A, B, C, and D are constants. The transverse field components E_θ and H_θ are obtained substituting (9) into (3). These field components together with E_z and H_z must be matched at the core boundary ($r = a$). Such conditions are expressed by the matrix equation

$$\begin{bmatrix} U_1(a) & U_2(a) & U_3(a) & 0 \\ V_1(a) & V_2(a) & 0 & U_3(a) \\ V_1'(a) + \sqrt{1-b}\,(m/a)U_1(a) & V_2'(a) + \sqrt{1-b}\,(m/a)U_2(a) & \sqrt{1-b}\,(m/a)U_3(a) & U_3'(a) \\ (1-\delta)U_1'(a) + \sqrt{1-b}\,(m/a)V_1(a) & (1-\delta)U_2'(a) + \sqrt{1-b}\,(m/a)V_2(a) & (1-\delta)U_3'(a) & \sqrt{1-b}\,(m/a)U_3(a) \end{bmatrix} \cdot \begin{bmatrix} A \\ B \\ C \\ D \end{bmatrix} = 0. \tag{10}$$

The condition that (10) possesses a nontrivial solution is that the determinant of the square matrix in (10) vanishes. This is alternatively written as

$$\left[\frac{U_3'(a)}{U_3(a)} - \frac{U_1'(a)}{U_1(a)}\right] \cdot \left[\frac{U_3'(a)}{U_3(a)} - \frac{V_2'(a)}{V_2(a)}\right] = \frac{V_1(a)}{U_1(a)} \cdot \frac{U_2(a)}{V_2(a)} \cdot \left[\frac{U_3'(a)}{U_3(a)} - \frac{U_2'(a)}{U_2(a)}\right] \cdot \left[\frac{U_3'(a)}{U_3(a)} - \frac{V_1'(a)}{V_1(a)}\right]. \tag{11}$$

This is the exact characteristic equation for determining β (or b).

III. Kurtz–Streifer Approximation

It may, in general, be difficult to obtain two sets of the exact solutions of (5), $\{U_1(r),V_1(r)\}$ and $\{U_2(r),V_2(r)\}$. However, if the index variation is sufficiently smooth, the field may be considered to be a locally plane wave. Under this assumption, the behaviors of electric ($U_i(r)$) and magnetic ($V_i(r)$) fields can be identified. Therefore, we can approximate, in (5), $\chi'/(1-\chi) \simeq 0$, $\sqrt{1-b} \simeq 1$, and $1/(1-\chi) \simeq 1$ [1], and obtain

$$\left\{\frac{d^2}{dr^2} + \left(\frac{1}{r} + \frac{\chi'}{b-\chi}\right)\frac{d}{dr} + k^2(b-\chi) - \frac{m^2}{r^2}\right\}\begin{Bmatrix} U(r) \\ V(r) \end{Bmatrix} = -m\left(\frac{\chi'}{b-\chi}\right)\frac{1}{r}\begin{Bmatrix} V(r) \\ U(r) \end{Bmatrix}. \tag{12}$$

Kurtz and Streifer [1] have showed that the solutions of (12) are given by (hereafter, the upper and lower signs correspond to $i = 1$ and 2, respectively)

$$U_i(r) = \pm V_i(r) = -\frac{1}{k}\left[\Phi_i'(r) + \frac{1 \mp m}{r}\Phi_i(r)\right], \quad i = 1,2$$

$$\Phi_i(r) = \frac{1}{k(b-\chi)}\left[U_i'(r) \pm \frac{m}{r}U_i(r)\right], \quad i = 1,2 \tag{13}$$

where $\Phi_i(r)$ is the bounded solution of

$$\Phi_i''(r) + \frac{1}{r}\Phi_i'(r) + \left[k^2(b-\chi) - \frac{(m \mp 1)^2}{r^2}\right]\Phi_i(r) = 0, \qquad i = 1,2. \quad (14)$$

This approximation is employed here; (13) is substituted into (11). Then we obtain[2]

$$S_0 \frac{\Phi_i'(a)}{\Phi_i(a)} = -R\left(\frac{a}{S_0}, \pm m\right), \qquad i = 1,2 \quad (15)$$

where S_0 is the eigenspot size of the medium ($\equiv \sqrt{a/k\sqrt{\delta}}$) and

$$R(x, \pm m) \equiv \left\{\frac{1 \mp m}{x} + \frac{k^2 S_0^2(b-\delta)}{S_0 \dfrac{U_3'(a)}{U_3(a)} \pm \dfrac{m}{x}}\right\}, \qquad i = 1,2. \quad (16)$$

IV. Determination of Propagation Constants

To obtain the propagation constants from the characteristic equation, the bounded solutions of (14) are substituted into (15). We see that such solutions are of the form [7]–[9]

$$\Phi_i(r) = \left(\frac{r}{S_0}\right)^{\alpha} e^{-(1/2)(r/S_0)^2} L_\nu^{(\alpha)}\left(\frac{r^2}{S_0^2}\right), \qquad i = 1,2 \quad (17)$$

where $L_\nu^{(\alpha)}(x)$ is the Laguerre function [9], and α and ν are defined by

$$\alpha \equiv |m \mp 1|, \qquad i = 1,2 \quad (18)$$

$$\nu \equiv \frac{1}{4}\left(\frac{ka}{\sqrt{\delta}}\right) b - \frac{1}{2}(\alpha + 1). \quad (19)$$

If the core medium is infinitely extended, the value of ν must be taken to be equal to an integer n [1]. This is a well-known fact in the theory of wave propagation in a parabolic-index medium [1]. In such a case, the Laguerre function is called the Laguerre polynomial of nth degree. In our case, ν is not equal to n; all the effects of the cladding are included in the deviation of ν from n, denoted by $\Delta\nu$,

$$\nu \equiv n + \Delta\nu. \quad (20)$$

The propagation characteristics can now be determined by studying the dependence of $\Delta\nu$ on the mode indices n and m. To express $\Delta\nu$ as a function of the core radius and the mode indices, we first try to decompose the bounded solution (17) as follows (Appendix I), using the field decomposition technique [5], [6].

$$\Phi_i(r) = \cos(\pi\nu) P_\nu^{(\alpha)}\left(\frac{r}{S_0}\right) - \sin(\pi\nu) Q_\nu^{(\alpha)}\left(\frac{r}{S_0}\right). \quad (21)$$

The explicit definition for the functions $P_\nu^{(\alpha)}(\xi)$ and $Q_\nu^{(\alpha)}(\xi)$, together with the physical interpretation and the mathematical derivation of (21), is given in Appendix I. The asymptotic aspects of these functions will be summarized.

1) $P_\nu^{(\alpha)}$ and $Q_\nu^{(\alpha)}$ are, respectively, a damped solution and a growing solution such that

$$P_\nu^{(\alpha)}(\xi) \to \frac{1}{\Gamma(\nu+1)} \xi^{2\nu+\alpha} e^{-(1/2)\xi^2}$$

$$Q_\nu^{(\alpha)}(\xi) \to \frac{1}{\pi}\Gamma(\nu+\alpha+1)\xi^{-2\nu-\alpha-2} e^{(1/2)\xi^2} \quad (22)$$

as $\xi \to \infty$, where Γ denotes the gamma function.

2) For $\nu \gg \alpha$ and $r < r_t$ where r_t is the turning point[3] ($= 2S_0\sqrt{\nu + (\alpha+1)/2}$, [2]), the complex solution $P_\nu^{(\alpha)} - jQ_\nu^{(\alpha)}$ represents the outgoing wave of the WKB type

$$P_\nu^{(\alpha)}\left(\frac{r}{S_0}\right) - jQ_\nu^{(\alpha)}\left(\frac{r}{S_0}\right) \sim S_\nu(r) \exp\left[-j\frac{\pi}{4} + jk\int_r^{r_t} \sqrt{b - \chi(t)}\, dt\right] \quad (23)$$

where the amplitude function $S_\nu(r)$ is

$$S_\nu(r) = \frac{\sqrt{8/\pi} \cdot \Gamma(\nu + \alpha + 1)}{\Gamma(\nu+1) \cdot \left(\nu + \dfrac{\alpha+1}{2}\right)^{\alpha/2} \cdot \sqrt{kr\sqrt{b - \chi(r)}}}. \quad (24)$$

Hence the complex conjugate wave $P_\nu^{(\alpha)} + jQ_\nu^{(\alpha)}$ is an incoming wave.

3) $P_\nu^{(\alpha)}$ and $Q_\nu^{(\alpha)}$ are the standing waves composed of the outgoing wave and the incoming wave under certain reflection conditions. The field behaviors of $P_\nu^{(\alpha)}$ and $Q_\nu^{(\alpha)}$ are shown in Fig. 2(a) and (b), respectively.

We substitute (21) into (15). Then

$$\cos(\pi\nu)[P_\nu^{(\alpha)\prime}(\xi_a) + R(\xi_a, \pm m)P_\nu^{(\alpha)}(\xi_a)] - \sin(\pi\nu)[Q_\nu^{(\alpha)\prime}(\xi_a) + R(\xi_a, \pm m)Q_\nu^{(\alpha)}(\xi_a)] = 0 \quad (25)$$

where $\xi_a \equiv a/S_0$. Furthermore, we substitute $\cos(\pi\nu) = (-1)^n \cos(\pi\Delta\nu)$ and $\sin(\pi\nu) = (-1)^n \sin(\pi\Delta\nu)$ into (25), noting that $|P_\nu^{(\alpha)}| \ll |Q_\nu^{(\alpha)}|$ and $n \gg |\Delta\nu|$ for large ξ_a. The alternative expression of the resulting equation is

$$\Delta\nu \simeq \left(\frac{1}{\pi}\right) \tan^{-1}\left[\frac{P_n^{(\alpha)\prime}(\xi_a) + R(\xi_a, \pm m)P_n^{(\alpha)}(\xi_a)}{Q_n^{(\alpha)\prime}(\xi_a) + R(\xi_a, \pm m)Q_n^{(\alpha)}(\xi_a)}\right], \qquad i = 1,2. \quad (26)$$

[2] By virtue of $U_i(r) = \pm V_i(r)$ [refer to (13)], (11) becomes

$$\frac{U_3'(a)}{U_3(a)} = \frac{U_i'(a)}{U_i(a)}, \qquad i = 1, 2.$$

Further, noting that $\chi = \delta$ at $r = a$ in (13), we can derive

$$\frac{U_i'(a)}{U_i(a)} \pm \frac{m}{a} = k(b-\delta)\frac{\Phi_i(a)}{U_i(a)} = -\frac{k^2(b-\delta)\Phi_i(a)}{\Phi_i'(a) + \left(\dfrac{1 \mp m}{a}\right)\Phi_i(a)}, \qquad i = 1, 2.$$

Both equations are used to eliminate the term $U_i'(a)/U_i(a)$. In this way, we obtain (15)

[3] The point at which the optical ray is reflected is called the turning point from the analogy of motion of a harmonic oscillator. The modes satisfying $r_t < a(r_t > a)$ are propagating modes (cutoff modes). Hence in our problem, $r_t < a$ is satisfied.

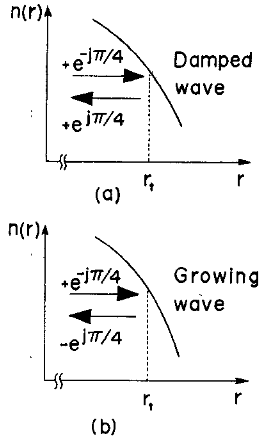

Fig. 2. Interpretation of the field continuity at the turning point r_t.

Obviously, this process of approximation allows us to replace the value of b in R by the approximate value,[4] $(2\sqrt{\delta}/ka)(2n + \alpha + 1)$. To calculate (26), the mathematical formulas for $P_n^{(\alpha)}(\xi)$ and $Q_n^{(\alpha)}(\xi)$ are cited from Appendix I.

$$P_n^{(\alpha)}(\xi) = \xi^{\alpha} e^{-(1/2)\xi^2} p_n^{(\alpha)}(\xi^2)$$
$$Q_n^{(\alpha)}(\xi) = \xi^{\alpha} e^{-(1/2)\xi^2} q_n^{(\alpha)}(\xi^2) \tag{27}$$

where

$$\left.\begin{matrix} p_n^{(\alpha)}(x) \\ q_n^{(\alpha)}(x) \end{matrix}\right\} = (-1)^n \frac{e^x}{n!} x^{-\alpha} \frac{d^n}{dx^n}\left[e^{-x}x^{n+\alpha}\left\{\begin{matrix} 1 \\ q_0^{(\alpha)}(x) \end{matrix}\right\}\right] \tag{28}$$

and

$$p_0^{(\alpha)}(x) = 1$$
$$p_1^{(\alpha)}(x) = x - 1 - \alpha$$
$$q_0^{(\alpha)}(x) = q_0^{(0)}(x) - \frac{e^x}{\pi}\sum_{l=0}^{\alpha-1}\frac{l!}{x^{l+1}}$$
$$q_1^{(\alpha)}(x) = p_1^{(\alpha)}(x)q_0^{(0)}(x) - \frac{e^x}{\pi} + \frac{e^x}{\pi}\sum_{l=0}^{\alpha-1}\frac{(\alpha - l)l!}{x^{l+1}}$$
$$q_0^{(0)}(x) = \frac{1}{\pi}\,\mathrm{l}i(e^x)$$
$$= \frac{1}{\pi}\left\{\gamma + \log x + x + \frac{x^2}{2\cdot 2!} + \frac{x^3}{3\cdot 3!} + \cdots\right\} \tag{29}$$

where the terms of $\sum$ are to be omitted when $\alpha = 0$, $\mathrm{l}i(x)$ is the logarithmic integral function [7], and γ is the Euler constant ($= 0.57721 \cdots$). It may be convenient to use the following recurrence formula when obtaining $q_n^{(\alpha)}(x)$ for $n \geq 2$:

$$q_n^{(\alpha)}(x) = -\frac{1}{n}\{(2n + \alpha - 1 - x)q_{n-1}^{(\alpha)}(x) + (n + \alpha - 1)q_{n-2}^{(\alpha)}(x)\}. \tag{30}$$

[4] The exact value of b, $(2\sqrt{\delta}/ka)(2\nu + \alpha + 1)$ [see (19)] is approximated. This approximation is not valid near the cutoff frequency. The value of $\Delta\nu$ of the TE_{01} mode at the cutoff frequency, which was obtained from the numerical analysis by Okoshi and Okamoto [11], is -0.118, whereas (26) yields -0.124.

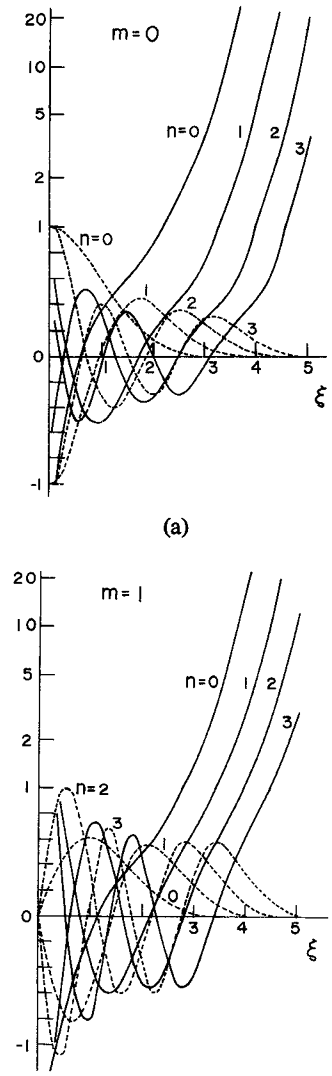

Fig. 3. Solutions $P_n^{(m)}(\xi)$ (dotted curves) and $Q_n^{(m)}(\xi)$ (solid curves) for various n. (a) $m = 0$. (b) $m = 1$.

We note that the same formula is applicable for $p_n^{(\alpha)}(x)$ $(= (-1)^n L_n^{(\alpha)}(x))$. Examples of $P_n^{(m)}(\xi)$ and $Q_n^{(m)}(\xi)$ are shown in Fig. 3(a) and (b).

As is seen from (4) and (19), the propagation constants can be calculated by

$$\beta = k\sqrt{1 - 4\left(\frac{\sqrt{\delta}}{ka}\right)\left(n + \Delta\nu + \frac{\alpha + 1}{2}\right)}, \qquad i = 1,2. \tag{31}$$

The value of $\Delta\nu$ is, in general, negative, so that the value of β becomes slightly large when the cladding exists.

When $m = 0$, (26) yields the same result for $i = 1$ and 2, and therefore the propagation constants of TE_{0l} and TM_{0l} modes ($l \equiv n + 1$) are the same. When $m \geq 1$, $i = 1$ and 2 correspond to HE_{ml} and EM_{ml} modes, respectively [3]. The negative values of $\Delta\nu$ for such modes are plotted in Fig. 4. If ξ_a is large compared with unity, it is possible to

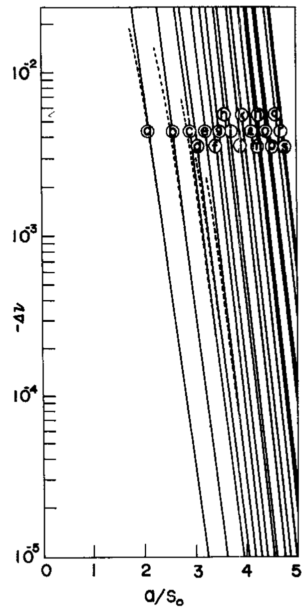

Fig. 4. The values of $-\Delta\nu$ for guided modes. The dotted curves indicate the first-order asymptotic solutions. a—HE_{11}, b—TE_{01}, TM_{01}, HE_{21}, c—EH_{11}, HE_{31}, d—HE_{12}, e—EH_{21}, HE_{41}, f—TE_{02}, TM_{02}, HE_{22}, g—EH_{31}, HE_{51}, h—EH_{12}, HE_{32}, i—HE_{13}, j—EH_{22}, HE_{42}, k—TE_{03}, TM_{03}, HE_{23}, l—EH_{32}, HE_{52}, m—EH_{13}, HE_{33}, n—HE_{14}, o—EH_{23}, HE_{43}, p—TE_{04}, TM_{04}, HE_{24}, q—EH_{33}, HE_{53}, r—EH_{14}, HE_{34}, s—HE_{15}.

express $\Delta\nu$ by the asymptotic form (Appendix II)

$$\Delta\nu \simeq -\frac{1}{4}\frac{\xi_a^{4n+2\alpha}}{n!\,(n+\alpha)!}\,e^{-\xi_a^2} \cdot \left\{1 - 2\,\frac{[(n-1)(n+\alpha-1) - 7/4]}{\xi_a^2}\right\}, \qquad i = 1,2. \quad (32)$$

The dotted curves in Fig. 4 indicate the asymptotic results computed from (32). These curves show that the asymptotic formula is a very good approximation of (26) unless the turning point is close to the core boundary.

V. Comparison with the Numerical Analysis

To check the validity of the field decomposition analysis presented here and the formula of $\Delta\nu$, we consider the propagation of the HE_{11}, TE_{01}, TM_{01}, HE_{21}, and EH_{11} waves in the lower order mode fiber whose core radius is chosen to be relatively small. The values of $\Delta\nu$ for these waves are compared with the numerical results by Ahmew [10]. The graphical data of Ahmew for the normalized propagation constants are translated into the numerical data of $\Delta\nu$, using the relation (31). Such data are $\Delta\nu = -0.021$ at $\xi_a = 1.75$ for the HE_{11} wave, $\Delta\nu = -0.023$ at $\xi_a = 2.25$ for the TE_{01}, TM_{01}, and HE_{21} waves, and $\Delta\nu = -0.062$ at $\xi_a = 2.5$ for the EH_{11} wave. On the other hand, the theoretical values of $\Delta\nu$ derived from (26) are -0.022, -0.023, and -0.058, respectively. These values are in good agreement with the numerical data.

VI. Conclusion

The propagation constants of the propagating modes along the cladded parabolic-index optical fiber have been presented in simple form, using the approximate core solution derived by the Kurtz-Streifer approximation. The field decomposition analysis has been employed to approximately solve the characteristic equation and to obtain the analytic solution. The validity of the present analysis has been checked by comparing the theoretical results presented in this paper and the numerical results by Ahmew.

Appendix I

Field Decomposition

We show that $\Phi_i(r)$ is decomposed into a damped wave and a growing wave which tend to zero and infinity as $r \to \infty$, respectively.

A. Physical Interpretation

To explain the physical significance of the field decomposition in the inhomogeneous medium from the asymptotic behavior of $\Phi_i(r)$, it is assumed that 1) the index variation is sufficiently smooth, and 2) the field variation in θ is sufficiently small compared with that in r ($\nu \gg \alpha$).

Now, for simplicity, we consider the special case of $\nu = n$. Then, if $r < r_t$, $\Phi_i(r)$ is given by the asymptotic form [2][5]

$$\Phi_i(r) \simeq \frac{2(n+\alpha)!}{n!\left(n + \frac{\alpha+1}{2}\right)^{\alpha/2}}\frac{1}{\sqrt{r}}\sqrt{\frac{u(r)}{u'(r)}}\,J'_{\alpha+1}(u(r)) \quad (A1)$$

where J denotes the Bessel function, the prime indicates differentiation, and

$$u(r) \equiv k\int_0^r \sqrt{b - \chi(t)}\,dt = \pi\left(n + \frac{\alpha+1}{2}\right) - k\int_r^{r_t}\sqrt{b-\chi(t)}\,dt. \quad (A2)$$

Applying the asymptotic formula, for large argument,

$$J'_{\alpha+1}(x) \simeq -\sqrt{\frac{2}{\pi x}}\sin\left(x - \frac{\pi}{2}\alpha - \frac{3}{4}\pi\right) \quad (A3)$$

to (A1), we obtain

$$\Phi_i(r) \sim S_n(r)\cos\left(n\pi + \frac{\pi}{4} - k\int_r^{r_t}\sqrt{b-\chi(t)}\,dt\right) \quad (A4)$$

where $S_n(r)$ is the amplitude function defined by (24).

[5] They gave the asymptotic solution with an arbitrary magnitude. The complete form is uniquely determined from the condition

$$\Phi_i(r) \to \frac{(n+\alpha)!}{n!\,\alpha!}\left(\frac{r}{S_0}\right)^\alpha, \qquad \text{as } r \to 0.$$

When $\nu \neq n$, the asymptotic form of $\Phi_i(r)$ may be given by an analytic continuation of (A4),

$$\Phi_i(r) \sim S_\nu(r)\cos\left(\pi\nu + \frac{\pi}{4} - k\int_r^{r_t}\sqrt{b-\chi(t)}\,dt\right) \quad \text{(A5)}$$

$$= \cos(\pi\nu)S_\nu(r)\cos\left(\frac{\pi}{4} - k\int_r^{r_t}\sqrt{b-\chi(t)}\,dt\right)$$

$$- \sin(\pi\nu)S_\nu(r)\sin\left(\frac{\pi}{4} - k\int_r^{r_t}\sqrt{b-\chi(t)}\,dt\right). \quad \text{(A6)}$$

In (A6), $\Phi_i(r)$ is decomposed into two waves. To inspect the behavior of these waves in the region such that $r > r_t$, the WKB theory [12] is used. This theory is illustrated in Fig. 2(a) and (b). Fig. 2(a) [Fig. 2(b)] shows that the wave which tends to $S_\nu(r)\cos(\pi/4 - 0)[S_\nu(r)\sin(\pi/4 - 0)]$, as $r \to r_t$ in the oscillatory region, will decay (grow) exponentially as $r \to \infty$. It can therefore be concluded that the first and second terms in the right-hand side of (A6) express the damped and growing waves, respectively. The wave $P_\nu^{(\alpha)} - jQ_\nu^{(\alpha)}$ is just the outgoing wave in Fig. 2(a) and (b).

B. Derivation from the Theory of Confluent Hypergeometric Functions

$P_\nu^{(\alpha)}(r/S_0)$ and $Q_\nu^{(\alpha)}(r/S_0)$ are two independent solutions of (14). Therefore, the functions defined by

$$p_\nu^{(\alpha)}(x) \equiv x^{-\alpha/2}e^{x/2}P_\nu^{(\alpha)}(\sqrt{x})$$

$$q_\nu^{(\alpha)}(x) \equiv x^{-\alpha/2}e^{x/2}Q_\nu^{(\alpha)}(\sqrt{x}) \quad \text{(A7)}$$

are two independent solutions of Laguerre's differential equation

$$xy''(x) + (\alpha + 1 - x)y'(x) + \nu y(x) = 0 \quad \text{(A8)}$$

and (21) is equivalent to

$$L_\nu^{(\alpha)}(x) = \cos(\pi\nu)p_\nu^{(\alpha)}(x) - \sin(\pi\nu)q_\nu^{(\alpha)}(x). \quad \text{(A9)}$$

From (22), $p_\nu^{(\alpha)}(x)$ and $q_\nu^{(\alpha)}(x)$ must be

$$p_\nu^{(\alpha)}(x) \to x^\nu/\Gamma(\nu+1)$$

$$q_\nu^{(\alpha)}(x) \to \Gamma(\nu+\alpha+1)e^x/\pi x^{\nu+\alpha+1} \quad \text{(A10)}$$

as $x \to \infty$. We prove that for $x > 0$, $\nu \geq 0$, and $\alpha = 0,1,2,3,\cdots$, such functions are given by

$$p_\nu^{(\alpha)}(x) = \frac{1}{2\pi j}\int_{C_1} t^{-\nu-1}(1-t)^{\nu+\alpha}e^{xt}\,dt \quad \text{(A11)}$$

$$q_\nu^{(\alpha)}(x) = \frac{1}{2\pi}\int_{C_2'+C_2''} t^{-\nu-1}(1-t)^{\nu+\alpha}e^{xt}\,dt \quad \text{(A12)}$$

where C_1, C_2', and C_2'' are the paths of integration on the t plane [see Fig. 5(a) and (b)], and $\arg t = \arg(1-t) = 0$ at the interval (0,1) of the real axis of the t plane.

Proof: We give the proof using the theory of confluent hypergeometric functions.

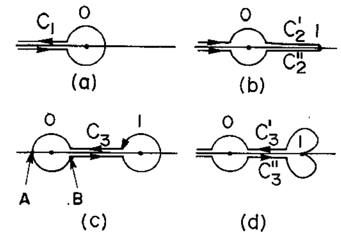

Fig. 5. The paths of integration on the t plane.

When α is an integer, the Laguerre function $L_\nu^{(\alpha)}(x)$ is expressed by [9, p. 268, eq. (37), and p. 272, eq. (3)][6]

$$L_\nu^{(\alpha)}(x) = \frac{\Gamma(\alpha+\nu+1)}{\alpha!\,\Gamma(\nu+1)}e^{x/2}x^{-(\alpha+1)/2}M_{\nu+(\alpha+1)/2,\alpha/2}(x) \quad \text{(A13)}$$

$$= -\frac{1}{2\pi j}\oint_{C_3}^{(0+,1+)}(-t)^{-\nu-1}(1-t)^{\nu+\alpha}e^{xt}\,dt \quad \text{(A14)}$$

$$= \frac{e^{-j\pi\nu}}{2\pi j}\oint_{C_3}^{(0+,1+)}t^{-\nu-1}(1-t)^{\nu+\alpha}e^{xt}\,dt \quad \text{(A15)}$$

where $M_{\kappa\mu}(x)$ is the Whittaker function [7] and the path C_3 is shown in Fig. 5(c) [in (A14), $\arg(-t) = \arg(1-t) = 0$ at the point A, and in (A15), $\arg t = \arg(1-t) = 0$ at the point B].

We decompose C_3 into C_3' and C_3'' [Fig. 5(d)]. Then, the integrals of (A15) on C_3' and C_3'' are written as

$$\int_{C_3''} = \int_{C_2''}$$

and

$$\int_{C_3'} = e^{j2\pi(\nu+\alpha)}\int_{-C_2'} = -e^{j2\pi\nu}\int_{C_2'}$$

where the negative sign of $-C_2'$ indicates that the integration is to be carried out in the opposite sense. Thus

$$L_\nu^{(\alpha)}(x) = \frac{e^{-j\pi\nu}}{2\pi j}\int_{C_3'+C_3''}$$

$$= \frac{e^{-j\pi\nu}}{2\pi j}\int_{C_2''} - \frac{e^{j\pi\nu}}{2\pi j}\int_{C_2'}$$

$$= \cos(\pi\nu)\frac{1}{2\pi j}\int_{C_2''-C_2'}$$

$$- \sin(\pi\nu)\frac{1}{2\pi}\int_{C_2''+C_2'}. \quad \text{(A16)}$$

[6] [9, eq. (37)] should be corrected as follows:

$$L_\nu^{(\alpha)}(x) = \frac{\Gamma(\alpha+\nu+1)}{\alpha!\,\Gamma(\nu+1)}\Phi(-\nu,\alpha+1,x).$$

Equation (A14) can be derived from the above definition and the Φ function in [9].

Noting that $C_2'' - C_2' = C_1$, we see that (A16) represents (A9).[7] It is easy to verify (A10), carrying out the integration of (A11) and (A12) on the dominant parts of the paths of integration which contribute significantly to the integrals (the derivation is omitted here).

Next, we prove (28). For $p_n^{(\alpha)}(x)$, (28) is evident from $p_n^{(\alpha)}(x) = (-1)^n L_n^{(\alpha)}(x)$; this is the alternative definition of the Laguerre polynomials [8], [9].

By means of the transformation $t = 1 - u/x$, we rewrite (A12) as

$$q_n^{(\alpha)}(x) = -\frac{e^x}{2\pi} x^{-\alpha} \int u^{n+\alpha}(x-u)^{-n-1} e^{-u}\, du$$
$$= (-1)^n \frac{1}{n!} e^x x^{-\alpha} \frac{d^n}{dx^n}\left[-\frac{1}{2\pi}\int \frac{u^{n+\alpha}}{x-u} e^{-u}\, du\right]. \quad \text{(A17)}$$

We use the relation $u^n = (x + u - x)^n = x^n + nx^{n-1} \cdot (u - x) + \cdots + (u - x)^n$. Then

$$\int \frac{u^{n+\alpha}}{x-u} e^{-u}\, du = \int \frac{u^\alpha}{x-u} e^{-u}(x^n + \cdots)\, du = x^n \int \frac{u^\alpha}{x-u} e^{-u}\, du + (\text{a polynomial of } x \text{ with degree } n-1).$$

The first term in the last line represents $-2\pi e^{-x} x^{n+\alpha} q_0^{(\alpha)}(x)$. This result is substituted into (A17). Since the polynomial appearing in the right-hand side vanishes by nth differentiation, we obtain

$$q_n^{(\alpha)}(x) = (-1)^n \frac{1}{n!} e^x x^{-\alpha} \frac{d^n}{dx^n}\left[e^{-x} x^{n+\alpha} q_0^{(\alpha)}(x)\right]. \quad \text{(A18)}$$

Finally, we give several important relations for $q_n^{(\alpha)}(x)$,

$$x q_n^{(\alpha)\prime}(x) = n q_n^{(\alpha)}(x) + (n+\alpha) q_{n-1}^{(\alpha)}(x), \qquad n \ge 1$$
$$q_n^{(\alpha)\prime}(x) = -q_{n-1}^{(\alpha)\prime}(x) + q_{n-1}^{(\alpha)}(x), \qquad n \ge 1$$
$$p_n^{(\alpha)}(x) q_n^{(\alpha)\prime}(x) - p_n^{(\alpha)\prime}(x) q_n^{(\alpha)}(x) = \frac{(n+\alpha)!}{n!}\frac{1}{\pi}\frac{e^x}{x^{\alpha+1}}, \qquad n \ge 0. \quad \text{(A19)}$$

Appendix II
Derivation of (32)

To derive (32), we use the asymptotic formulas

$$p_n^{(\alpha)}(x) \simeq \frac{1}{n!}\left[x^n - n(n+\alpha)x^{n-1}\right] \quad \text{(A20)}$$

$$q_n^{(\alpha)}(x) \simeq \frac{(n+\alpha)!}{\pi}\frac{e^x}{x^{n+\alpha+1}}\left[1 + \frac{(n+1)(n+\alpha+1)}{x}\right] \quad \text{(A21)}$$

$$x\frac{K_m'(x)}{K_m(x)} \simeq -x - \frac{1}{2} - \frac{(4m^2-1)}{8}\frac{1}{x} \quad \text{(A22)}$$

and

$$R(\xi_a, \pm m) \simeq 1/2\xi_a + \sqrt{\xi_a^2 - 2(2n+\alpha+1)} + (\pm 2m - 1)(\pm 2m - 3)/8\xi_a^3$$
$$\simeq \xi_a - (2n + \alpha + 1/2)/\xi_a - [(2n+1)(n+\alpha+1/2) + 1/8]/\xi_a^3. \quad \text{(A23)}$$

Therefore,

$$P_n^{(\alpha)\prime}(\xi_a) + R(\xi_a, \pm m) P_n^{(\alpha)}(\xi_a) \simeq -\frac{1}{2}\frac{e^{-(1/2)\xi_a^2}}{n!}\xi_a^{2n+\alpha-1} \cdot \left[1 - \frac{(n-2)(n+\alpha) - 2n - \frac{5}{4}}{\xi_a^2}\right] \quad \text{(A24)}$$

$$Q_n^{(\alpha)\prime}(\xi_a) + R(\xi_a, \pm m) Q_n^{(\alpha)}(\xi_a) \simeq \left(\frac{2}{\pi}\right)(n+\alpha)!\frac{e^{(1/2)\xi_a^2}}{\xi_a^{2n+\alpha+1}} \cdot \left[1 + \frac{n(n+\alpha) - \frac{1}{4}}{\xi_a^2}\right]. \quad \text{(A25)}$$

Substituting (A24) and (A25) into (26) and approximating the resulting equation, we obtain (32).

[7] Using the Whittaker function $W_{\kappa\mu}(x)$ [7], $p_\nu^{(\alpha)}(x)$ can also be written as

$$p_\nu^{(\alpha)}(x) = \frac{1}{\Gamma(\nu+1)} e^{(x/2)} x^{-(\alpha+1)/2} W_{\nu+(\alpha+1)/2, \alpha/2}(x).$$

References

[1] C. N. Kurtz and W. Streifer, "Guided waves in inhomogeneous focusing media, Pt. I: Formulation, solution for quadratic inhomogeneity," *IEEE Trans. Microwave Theory Tech.*, vol. MTT-17, pp. 11–15, Jan. 1969.

[2] ——, "Guided waves in inhomogeneous focusing media, Pt. II: Asymptotic solution for general weak inhomogeneity," *IEEE Trans. Microwave Theory Tech.*, vol. MTT-17, pp. 250–253, May 1969.

[3] G. L. Yip and S. Nemoto, "The relations between scalar modes in a lens-like medium and vector modes in a self-focusing optical fiber," *IEEE Trans. Microwave Theory Tech.* (Short Papers), vol. MTT-23, pp. 260–263, Feb. 1975.

[4] R. Yamada and Y. Inabe, "Guided waves along graded index dielectric rod," *IEEE Trans. Microwave Theory Tech.* (Letters), vol. MTT-23, pp. 813–814, Aug. 1974.

[5] M. Hashimoto, "The effect of an outer layer on propagation in a parabolic-index optical waveguide," *Int. J. Electron.*, vol. 39, no. 5, pp. 579–582, 1975.

[6] ——, "Propagation of cladded inhomogeneous dielectric waveguides," *IEEE Trans. Microwave Theory Tech.*, vol. MTT-24, pp. 404–409, July 1976.

[7] E. T. Whittaker and G. N. Watson, *A Course of Modern Analysis.* London: Cambridge, 1963.

[8] N. N. Lebedev, *Special Functions and Their Applications* (translated by R. A. Silverman). New Jersey: Prentice-Hall, 1965, ch. 4, p. 87.

[9] A. Erdelyi, W. Magnus, F. Oberhettinger, and F. G. Tricomi, *Higher Transcendental Function*, vol. I. New York: McGraw-Hill, 1953, p. 268.

[10] Y. H. Ahmew, "Propagation characteristics of the self-focusing fiber waveguide," M.S. thesis, McGill Univ., Montreal, Canada, Aug. 1973.

[11] T. Okoshi and K. Okamoto, "Analysis of wave propagation in inhomogeneous optical fibers using a variational method," *IEEE Trans. Microwave Theory Tech.*, vol. MTT-22, pp. 938–945, Nov. 1974.

[12] P. M. Mose and H. Feshbach, *Methods of Theoretical Physics, Pt. II.* New York: McGraw-Hill, 1953, ch. 9, p. 1095.